Surgical Neurology International

SNI: Spine, a supplement to Surgical Neurology International

OPEN ACCESS

For entire Editorial Board visit : http://www.surgicalneurologyint.com

Editor: Nancy E. Epstein, MD Winthrop University Hospital, Mineola, NY, USA

A blast from the past!: The value of adding single slice magnetic resonance myelography sequence to magnetic resonance imaging of the spine; a flashback to the conventional myelography of the past

Santosh Rai P. V., K. Santosh, Shrijeet Chakraborti[1], Shivananda Pai[2], Ishwara Keerthi[3], Muralidhar K. Pai[4]

Departments of Radiodiagnosis, [1]Pathology, [2]Neurology, [3]Spine Surgery, and [4]Neurosurgery, Kasturba Medical college, Manipal University, Mangalore, Karnataka, India

E-mail: *Santosh Rai P. V. - radiorai@gmail.com; K. Santosh - kondapalli99@hotmail.com; Shrijeet Chakraborti - shrijeet_chak@yahoo.co.in; Shivananda Pai - dshivanandpai@gmail.com; Ishwara Keerthi - drishwarak@gmail.com; Muralidhar K. Pai - drkmpai@gmail.com
*Corresponding author

Received: 10 August 13 Accepted: 16 September 14 Published: 30 December 14

This article may be cited as:
Santosh Rai PV, Santosh K, Chakraborti S, Pai S, Keerthi I, Pai MK. A blast from the past!: The value of adding single slice magnetic resonance myelography sequence to magnetic resonance imaging of the spine; a flashback to the conventional myelography of the past. Surg Neurol Int 2014;5:S523-8.
Available FREE in open access from: http://www.surgicalneurologyint.com/text.asp?2014/5/16/523/148018

Abstract

Background: The study was undertaken to determine whether a single slice magnetic resonance (MR) myelogram sequence improves the interpretation and diagnostic yield for magnetic resonance imaging (MRI) of the spine.

Methods: A total of 100 cases with positive findings were retrospectively reviewed. All patients had initial imaging with sagittal T1-weighted (T1-W) and T2-weighted (T2-W) scans, followed by axial T2-W images. Subsequently, a heavily T2-W single slice MR myelogram sequence was acquired in coronal and sagittal planes. The MR myelogram images were evaluated initially by a radiologist, and, further independently reviewed, by a neurologist, neurosurgeon, and spine surgeon. The utility of the MR myelogram in establishing the diagnosis was graded on a 4-point scale.

Results: Out of 100 cases, 53% showed degenerative spine or disc disease, 14% space occupying lesions, 13%, congenital lesions, 7% infection, and 7% other conditions. The MR myelogram contributed additional information in 50-74% cases. The intraclass correlation coefficient showed overall good agreement between observers in grading the utility of MR myelogram.

Conclusion: Single slice MR myelography is noninvasive avoiding the complications associated with lumbar punctures/intrathecal contrast injections, while image acquisition takes only an added 6-8 s. Although MR myelogram has no value as a stand-alone sequence, its inherent advantage is that it completes the overview of the spinal pathology in entirety, and adds vital three-dimensional information in 50-74% of cases.

Key Words: Magnetic resonance imaging, magnetic resonance myelography, myelogram, spine

Access this article online

Website: www.surgicalneurologyint.com

DOI: 10.4103/2152-7806.148018

Quick Response Code:

INTRODUCTION

Noncontrast magnetic resonance (MR) myelography is a noninvasive technique that can provide anatomic information about the subarachnoid space. Major advantages over conventional radiographic myelography include the lack of ionizing radiation, the avoidance of lumbar puncture/intrathecal contrast material.[9] This study was designed to determine whether single-slice MR myelography would improve the interpretation and diagnostic yield of magnetic resonance imaging (MRI) of the spine.

MATERIALS AND METHODS

In 2013, 100 patients with back pain or spinal radicular symptoms and abnormal MRI findings were referred for evaluation. All patients had initial sagittal T1-weighted (T1-W) and T2-weighted (T2-W) scans, followed by axial T2-W images with a 1.5 T MRI scanner (Siemens MAGNETOM Avanto 1.5 Tesla MRI system) using a phased array spine coil. Subsequently a heavily T2-W half-Fourier acquisition single-shot turbo spin-echo (HASTE) single slice MR myelogram sequence with a field of view (FOV) of 280-300 mm and slab thickness of 50 mm, TR-8000, TE-1000 was acquired in each case in coronal and sagittal planes. High resolution thin T2-W images were acquired in specific pathologies.

Four reviewers of MR myelography

The MR and MR myelogram images (sagittal and axial planes) were initially evaluated by a radiologist and subsequently, independently, by a neurologist, neurosurgeon, and spine surgeon who all graded the findings based on a 4-point scale [Table 1]. Statistical analysis was done using intraclass correlation coefficient ($P = 0.000$), using SPSS (version 11.5).

Table 1: 4-point grading scale

Grade	Description
0	Contributed no additional information
1	Contributed no additional information but gave a visual impression
2	Contributed some additional information but not essential for diagnosis
3	Contributed some additional information which is essential for diagnosis
4	Contributed additional information not provided by conventional sequences

Table 2: Distribution of cases

Pathology	Number of cases
Congenital	
Scoliosis	7
Conjoined nerve roots	1
Diastematomyelia	1
Syringohydromyelia	2
Caudal regression syndrome	1
Spinal dysraphism	1
Degenerative spine/disc disease	
No significant disc disease	3
Mild disc bulges	20
Disc herniation including protrusion and extrusion	22
Sequestration	3
Facetal pathology	2
Perineural cysts	3
Vascular malformations within the thecal sac	2
Infective pathology	
Discitis	3
Tuberculosis in the paraspinal region	4
Spinal trauma	
Vertebral collapse	2
Brachial plexus root avulsion trauma	2
Space occupying lesions	
Intradural extramedullary tumors	4
Intramedullary tumors	2
Extramedullary tumors	7
Intramedullary cysts	1
Incidental extraspinal findings like pleural effusion, hydronephrosis, retroperitoneal nodes	4
Inflammatory polyneuropathy	1
Acquired Syringomyelia	2
Total	100

RESULTS

Distribution of pathology

Among the 100 cases, there were 53 cases of degenerative spine or disc disease, 14 of space occupying lesions, 13 of congenital lesions, 7 of infective pathology, 4 of spinal cord trauma (4%), and other conditions [Table 2].

Observer grading

The observers found that the inherent advantage of MR myelogram is the vital three-dimensional (3D) overview it provides. The distribution of grading score among the observers is tabulated in Table 3. All the four observers graded the utility of MR myelogram as grade 2 in 48-74% cases. The MR myelogram contributed some additional information, which is essential for diagnosis (grade 3) in up to 30% cases. In none of the pathologies did the grading reach grade 4, except in two cases, as graded by the neurologist [Table 3]. The intraclass correlation coefficient showed good overall agreement [Table 4] between the observers.

DISCUSSION

Based on slice selection, two techniques are currently in use: Multi-slice MR myelography and single-slice MR myelography. Single-slice MR myelography is performed

Table 3: Distribution of grading score among the observers

	Radiologist grading	Spine surgeon grading	Neurologist grading	Neurosurgeon grading
Grade 0				
No. of cases	3	5	4	3
%	3.0	5.0	4.0	3.0
Grade 1				
No. of cases	20	17	35	7
%	20.0	17.0	35.0	7.0
Grade 2				
No. of cases	67	48	51	74
%	67.0	48.0	51.0	74.0
Grade 3				
No. of cases	10	30	8	16
%	10.0	30.0	8.0	16.0
Grade 4				
No. of cases	0	0	2	0
%	0	0	2.0	0
Total				
No. of cases	100	100	100	100
%	100.0	100.0	100.0	100.0

Table 4: Agreement between observers

Pairs	Intraclass correlation coefficient	*P*
Spine surgeon grading-radiologist grading	0.619	0.000
Neurologist grading-radiologist grading	0.757	0.000
Neurosurgeon grading-radiologist grading	0.811	0.000
Neurologist grading-spine surgeon grading	0.681	0.000
Neurosurgeon grading-spine surgeon grading	0.787	0.000
Neurosurgeon grading-neurologist grading	0.718	0.000

Interpretation of intraclass correlation coefficient: <0.4: Poor, 0.4-0.75: Fair, 0.75-0.85: Good, >0.85: Excellent agreement

using a single thick slice and requires no postprocessing and provides a projection image with excellent suppression of background signals.[5] Single-slice MR myelography yields extremely heavy T2-W HASTE sequence images with excellent signal contrast, high spatial resolution and less artifact arising from cerebrospinal fluid (CSF) flow than seen on multi-slice MR myelography.

Single-slice MR myelography provides a fluoroscopic view similar to that of a conventional radiographic myelogram. Single-slice MR myelography can provide an overview of the thecal sac, even in the presence of a spinal block due to spinal stenosis or intrathecal adhesion, which results in a myelographic block on radiographic or CT myelography.[14]

Multi-slice MR myelography requires a relatively long imaging time. The image quality is often degraded by artifacts arising from CSFs pulsatile flow and background signal contributed by fat or paravertebral veins. Reconstructed images created using maximum intensity projection can obscure small intrathecal structures that are surrounded by hyperintense CSF.[7-9,11]

Because its imaging time is much shorter than that of multi-slice techniques, single-slice MR myelography can be readily added to a routine MR examination of the spine.

Single slice MR myelography is advantageous in documenting multiple pathologies. Similar studies performed on the subject have depicted a wide variety of pathologies of the spine represented exquisitely on the MR myelogram sequences establishing its role as a valuable sequence.[1,12]

A pictorial essay representation of the various pathologies seen in our collection of MR myelograms are presented below. Thecal sac filled with CSF shows markedly high signal intensity, whereas intrathecal structures such as spinal cord, nerve roots, and vessels are imaged as filling defects outlined by hyperintense CSF, whose margins appear smooth and clear [Figure 1]. They readily demonstrate conjoined nerve root and perineural or Tarlov's cysts [Figure 2]. Congenital lesions, such as meningocoeles, dural ectasia, diastematomyelia, syrinx, dermal sinuses, and complex syrinxes, and arterio-venous malformation (AVM) [Figure 3], intramedullary cord tumors and spinal stenosis, and pseudomeningocele [Figures 4-6], were well delineated in this sequence. Other pathologies, such as chronic inflammatory demyelinating disease (CIDP) [Figure 7], infections (e.g, tuberculosis [TB], pyogenic spondylo-discitis), scoliosis, extraspinal disease, and collections [Figures 8-10], were detectable.

Magnetic resonance myelography provides a visual impression in evaluation of cervical and lumbar spondylosis.[2,3,15] Redundant nerve roots associated with severe spinal stenosis may be seen as tortuous, elongated nerve roots proximal to the block in the lumbar region.[10]

Conjoined nerve roots, syringohydromyelia, intraspinal AVM, caudal regression and posttraumatic nerve root injuries, were typical examples where the MR myelography scored highly on the diagnostic utility scale and it had tremendous impact on the final diagnosis. MRI has generally replaced CT myelography as the primary diagnostic tool because of its noninvasiveness, less time and resource intensive, and because there is no exposure to ionizing radiation.[1,5,12,13] Although the findings of single-slice MR myelography such as intrathecal abnormal filling defects and contour abnormalities of thecal sac margin may not be specific, but when combined with conventional MR images they can help characterize and diagnose the lesions specifically.

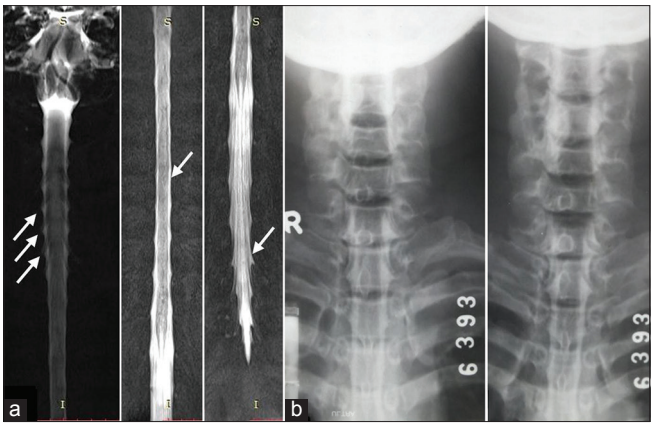

Figure 1: Coronal MR myelograms images of the cervical (a-i) and thoracic (a-ii) and lumbar (a-iii) spinal canals, which show nerve roots and vessels are imaged as filling defects (white arrows) outlined by hyperintense cerebrospinal fluid, whose margins appear smooth and clear. For comparison, conventional myelograms of the cervical thecal sac from the archives are displayed (b-i and b-ii)

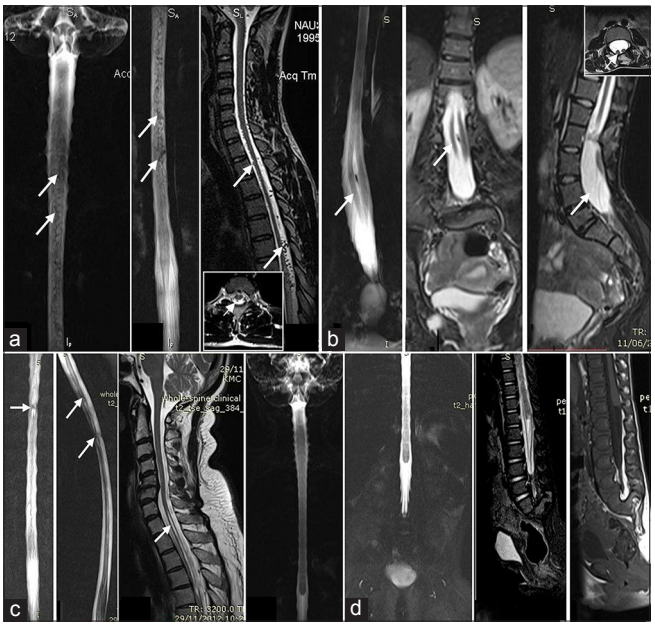

Figure 3: Coronal MR myelograms (a-i, a-ii) show engorged vascular channels as sepentine filling defects overlying the cord in thoracolumbar region also confirmed on sagittal T2 and axial T2 (a-iii) suggesting spinal arterio-venous malformation. Coronal MR myelogram (b-i) shows first look detection of dural ectasia in lumbosacral region with diastematomyelia in a 22-year-old female (b-ii, b-iii). Coronal and sagittal MR myelograms show simultaneous first look detection of syrinx with thinning of cord at cervicothoracic level confirmed at the sagittal T2 (c-iii white arrows) in a 55-year-old. Coronal MR myelograms show blunting of the conus (d-i, d-ii) in a patient of caudal regression syndrome (d-iii, d-iv)

Limitations

The degree of the spinal stenosis can be over-estimated on single-slice MR myelography because of relatively low signal-to-noise ratio. These images are of limited value for lateral and far lateral disc protrusions, disc impressions at the L5-S1 level and delineation of foraminal nerve root impingement [Figure 11].

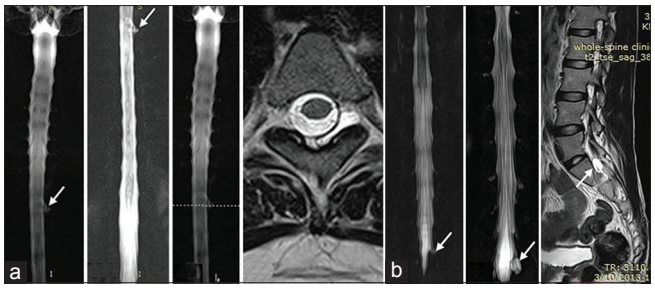

Figure 2: Coronal MR myelograms images (a-i, a-ii) shows perineural or Tarlov's cyst, which appear as cystic dilatation of proximal nerve root sleeve (white arrows); axial T2 section of the same level (a-iii, a-iv) shows the cyst as saccular hyperintense structure beside the thecal sac. Coronal MR myelogram images (b-i, b-ii) shows Conjoined nerve roots (white arrows) in a 39-year-old patient and Cystic dilatation of nerve root sleeves in 74-year-old female

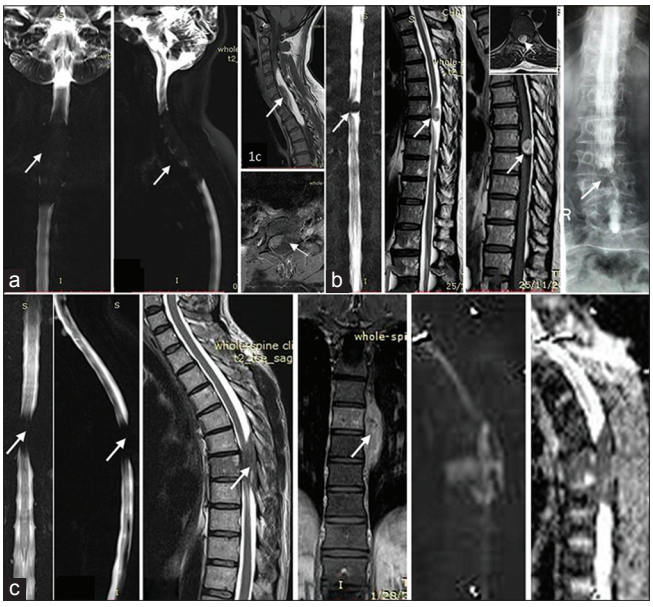

Figure 4: Coronal and sagittal myelography (a-i, a-ii) shows simultaneous first look impression of an intramedullary and intradural mass in the cervicothoracic region; which is confirmed on conventional MRI imaging (white arrows a-iii) as an enhancing fat containing intramedullary lesion suggesting dermoid. Coronal MR myelogram (b-i, b-ii) shows well defined intradural and extramedullary lesion at mid thoracic level on left side in a 55-year-old female confirmed as showing intense enhancement displacing cord right antero laterally and significantly compressing it at the T7-T8 level (white arrows). For comparison, a conventional myelogram from the archives shows IDEM. Coronal MR myelogram (c-i, c-ii) shows extradural lesion at mid thoracic level on left side and conventional sequences show uniformly enhancing extradural lesion (ciii, c-iv) showing restriction on DWI (c-v, c-vi) – Lymphoma in a 52-year-old male

In more recent studies, 3D MR myelography has been compared with radionuclide cisternography, and has been found useful in CSF leaks and reserved only for equivocal cases.[16] High resolution CT myelograms[4] have been employed to detect CSF leaks, which is a limitation of MR myelograms. 3D MR myelograms using fusion technique and volumetry have been studied and are found comparable to the gold standard, that is, postmyelography CT.[6]

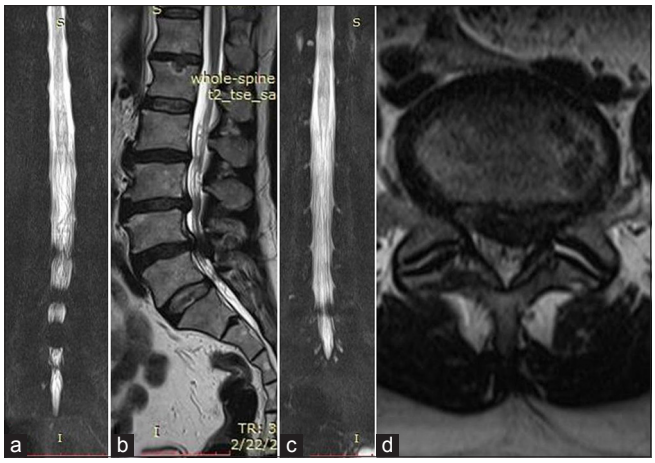

Figure 5: Coronal MR myelogram (a) shows degenerative spinal stenosis with redundant nerve roots in 74-year-old male as extrinisic impressions. Disc disease is shown on the sagittal T2 image (b). Coronal MR myelogram (c) shows single disc level disease compressing on the roots (d) as seen also on the axial T2 image in a 50-year-old patient

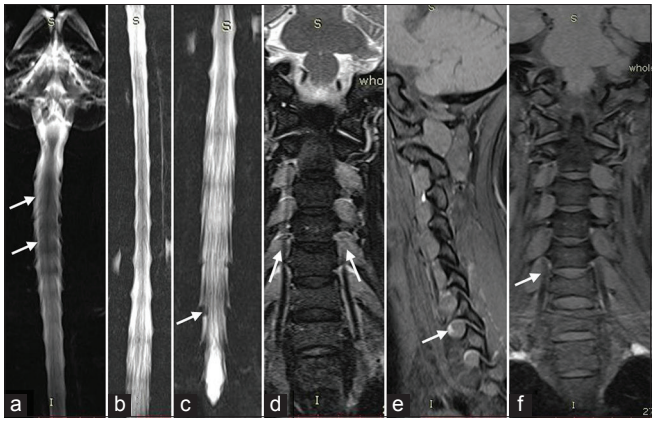

Figure 7: Coronal MR myelograms (a-c) showing predominantly extradural spinal nerve root thickening confirmed on the postcontrast coronal (d and f), sagittal (e) suggesting chronic inflammatory demyelinating disease

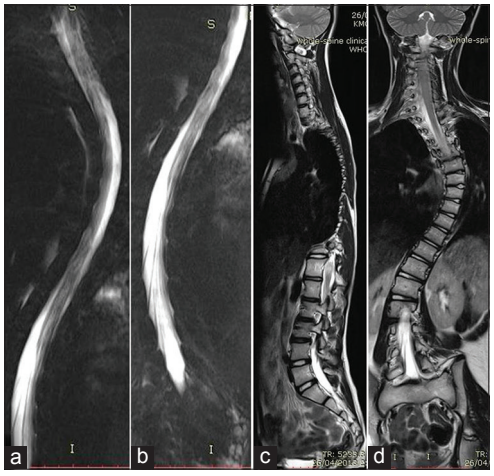

Figure 9: Coronal thick slab MR myelogram (a, b) displays the entire cord and thecal sac in one plane and gives a dimensional view. Conventional sagittal (c) and coronal images (d) do not display the entire spinal canal in a single plane unless technically corrected and fused

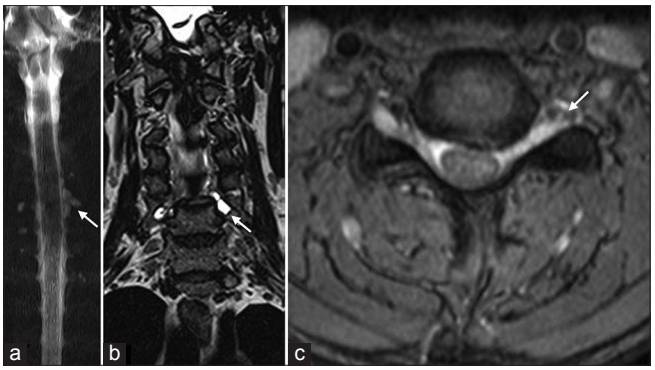

Figure 6: Coronal MR myelography (a) raises suspicion of pseudomeningocele as abnormal areas (white arrows), which are depicted as a tubular or oval cystic mass protruding from the thecal sac into the neural foramen extending into the paravertebral space (coronal T2 and axial T2 images – b, c)

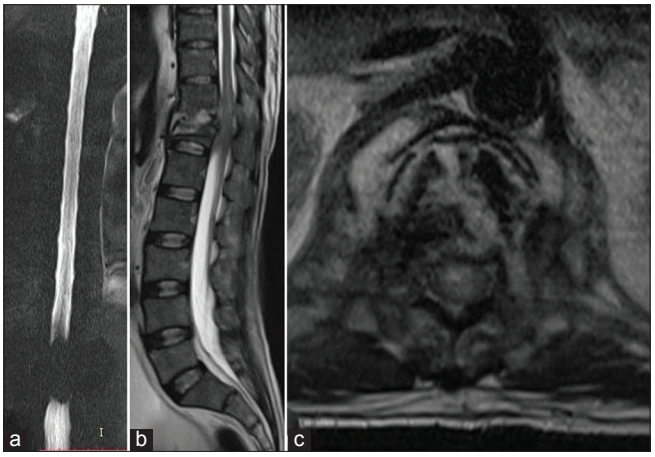

Figure 8: Coronal MR myelogram shows extrinsic compression on thecal sac (a) due to spondylodiscitis of tuberculosis (b, c)

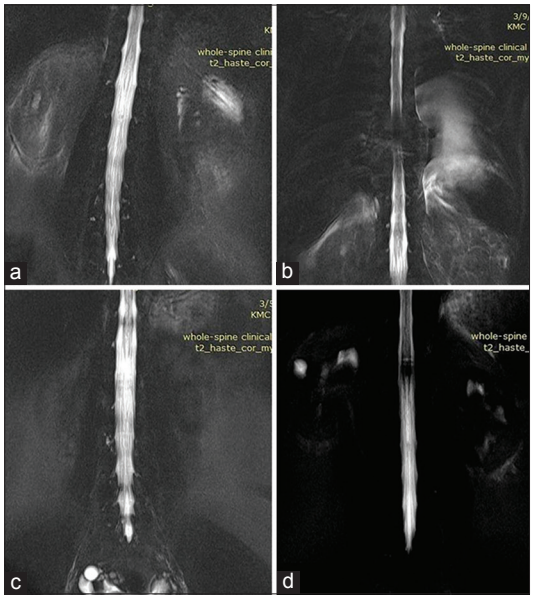

Figure 10: Coronal MR thick slabs incidentally demonstrate extra spinal findings like perinephric collections (a), pleural effusions (b), ovarian cysts (c) and hydronephrosis

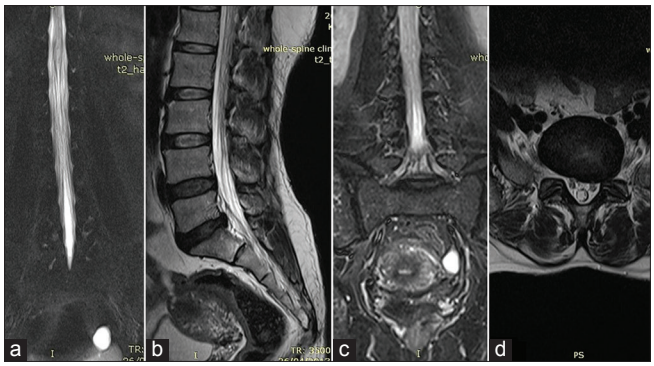

Figure 11: Limitation of MR myelography. Lateral and far lateral disc protrusions (a) are underestimated on the MR myelography and L5-S1 (b-d) disc impressions are underestimated

CONCLUSION

Single-slice MR myelography is a noninvasive method requiring neither lumbar puncture nor contrast medium, contributes an additional 50-74% of information toward establishing a diagnosis, while providing essential diagnostic information in 8-30% cases. It requires only an additional 6-8 s, and can therefore be performed even in busy imaging centers.

REFERENCES

1. Aggarwal A, Azad R, Ahmad A, Arora P, Gupta P. Additional merits of Two – dimensional Single thick slice Magnetic Resonance Myelography in Spinal Imaging. J Clin Imaging Sci 2012;2:84.
2. Boutin RD, Steinbach LS, Finnesey K. MR Imaging of degenerative diseases in the cervical spine. Magn Reson Imaging Clin N Am 2000;8:471-90.
3. Birchall D, Connelly D, Walker L, Hall K. Evaluation of magnetic resonance myelography in the investigation of cervical spondylotic radiculopathy. Br J Radiol 2003;76:525-31.
4. Chu E, MaAuliffe W. Use of flat panel DynaCT myelography to locate the site of CSF leak. J Med Imaging Radiat Oncol 2013;57:455-9.
5. Demaerel P, Bosmans H, Wilms G, Aerts P, Gaens J, Goffin J, *et al*. Rapid lumbar spine MR myelography using rapid acquisition with relaxation enhancement. AJR Am J Roentgenol 1997;168:377-8.
6. Eberhardt K, Ganslandt O, Stadlbauer A. Improved magnetic resonance myelography using image fusion. Rofo 2013;185:333-9.
7. el Gammal T, Brooks BS, Freedy RM, Crews CE. MR myelography: Imaging findings. AJR Am J Roentgenol 1995;164:173-7.
8. el Gammal TA, Crews CE. MR myelography of the cervical spine. Radiographics 1996;16:77-88.
9. Figueroa RE, Stone JA. MR imaging of degenerative spine disease: MR myelography and imaging of the posterior spinal elements. In: Castillo M, editor. Spinal imaging, State of Art. Philadelphia: Hanley and Belfus; 2001. p. 105-22.
10. Hacker DA, Latchaw RE, Yock DH Jr, Ghosharjura K, Gold LH. Redundant lumbar nerve root syndrome: Myelographic features. Radiology 1982;143:457-61.
11. Krudy AG. MR myelography using heavily T2-weighted fast spin-echo pulse sequences with fat presaturation. AJR Am J Roentgenol 1992;159:1315-20.
12. Nagayama M, Watanabe Y, Okumura A, Amoh Y, Nakashita S, Dodo Y. High-resolution single-slice MR myelography. AJR Am J Roentgenol 2002;179:515-21.
13. O'Connell MJ, Ryan M, Powell T, Eustace S. The value of routine MR myelography at MRI of the lumbar spine. Acta Radiol 2003;44:665-72.
14. Quencer RM, Morse BM, Green BA, Eismont FJ, Brost P. Intraoperative spinal sonography: Adjunct to metrizamide CT in the assessment and surgical decompression of post-traumatic spinal cord cysts. AJNR Am J Neuroradiol 1984;142;594-601.
15. Shafaie FF, Wippold FJ 2nd, Gado M, Pilgram TK, Riew KD. Comparison of computed tomography myelography and magnetic resonance imaging in the evaluation of cervical spondylotic myelopathy and radiculopathy. Spine (Phila Pa 1976) 1999; 24:1781-5.
16. Tomoda Y, Korogi Y, Aoki T, Morioka T, Takahashi H, Ohno M, *et al*. Detection of cerebrospinal fluid leakage: Initial experience with three-dimensional fast spin-echo magnetic resonance myelography. Acta Radiol 2008;49:197-203.